Journal of the European Ceramic Society xxx (2017) xxx–xxx

Contents lists available at www.sciencedirect.com

Journal of the European Ceramic Society

journal homepage: www.elsevier.com/locate/jeurceramsoc

# Preparation, characterization, and giant dielectric permittivity of ($Y^{3+}$ and $Nb^{5+}$) co–doped $TiO_2$ ceramics

Theeranuch Nachaithong[a,b], Wattana Tuichai[c], Pinit Kidkhunthod[d], Narong Chanlek[d], Prasit Thongbai[b,c,*], Santi Maensiri[e]

[a] Materials Science and Nanotechnology Program, Faculty of Science, Khon Kaen University, Khon Kaen 40002, Thailand
[b] Nanotec-KKU Center of Excellence on Advanced Nanomaterials for Energy Production and Storage, Khon Kaen 40002, Thailand
[c] Integrated Nanotechnology Research Center (INRC), Department of Physics, Faculty of Science, Khon Kaen University, Khon Kaen 40002, Thailand
[d] Synchrotron Light Research Institute (Public Organization), 111 University Avenue, Muang District, Nakhon Ratchasima 30000, Thailand
[e] Institute of Science, School of Physics, Suranaree University of Technology, Nakhon Ratchasima 30000, Thailand

ARTICLE INFO

*Article history:*
Received 16 January 2017
Received in revised form 8 April 2017
Accepted 17 April 2017
Available online xxx

*Keywords:*
Giant dielectric permittivity
Impedance spectroscopy
rutile–$TiO_2$
non-Ohmic properties
electrical properties

ABSTRACT

The microstructure and giant dielectric properties of $Y^{3+}$ and $Nb^{5+}$ co–doped $TiO_2$ ceramics prepared via a chemical combustion method are investigated. A main rutile–$TiO_2$ phase and dense ceramic microstructure are obtained in $(Y_{0.5}Nb_{0.5})_xTi_{1-x}O_2$ ($x$ = 0.025 and 0.05) ceramics. Nb dopant ions are homogeneously dispersed in the microstructure, while a second phase of $Y_2O_3$ particles is detected. The existence of $Y^{3+}$, $Nb^{5+}$, $Ti^{4+}$ and $Ti^{3+}$ as well as oxygen vacancies is confirmed by X–ray photoelectron spectroscopy and X–ray absorption near edge structure analysis. The sintered ceramics exhibit very high dielectric permittivity values of $10^4$–$10^5$ in the frequency range of 40–$10^6$ Hz. A low loss tangent value of ≈0.08 is obtained at 40 Hz. $(Y_{0.5}Nb_{0.5})_xTi_{1-x}O_2$ ceramics can exhibit non–Ohmic behavior. Using impedance spectroscopy analysis, the giant dielectric properties of $(Y_{0.5}Nb_{0.5})_xTi_{1-x}O_2$ ceramics are confirmed to be primarily caused by interfacial polarization.



## 1. Introduction

Giant dielectric oxides are material that exhibit very large dielectric permittivity ($\varepsilon'$) values, on the order of $10^3$–$10^6$, in the radio frequency range. These oxides have had a great impact on the progress made in recent years in the electronics industry, especially in high–energy–density storage devices. Many kinds of giant dielectric materials (e.g., oxides in a family of $\mathbf{A}Cu_3Ti_4O_{12}$ (where the A–site is occupied by cations with an average valance of +2) [1–5], $\mathbf{A}Fe_{1/2}\mathbf{B}_{1/2}O_3$ (**A** = Ba, Sr, Ca; **B** = Nb, Ta, Sb) [6–8], and $La_{2-x}Sr_xNiO_4$ [9–11] among others) were discovered and have been intensively investigated. All giant dielectric oxides show fascinating dielectric behaviors, and studies of their properties have led to insights into their underlying mechanisms. Both classical and elegant new models have been proposed to answer questions about why these oxides show giant dielectric behaviors. These models include the internal or surface barrier layer capacitor model (IBLC or SBLC) [4,12–15], nano–barrier layer capacitor model [16], small polaron hopping model [9,11], and the mixed–valent structure model [3,17] as well as the non–Ohmic sample–electrode contact model [15].

Unfortunately, unacceptably large values of the loss tangent (tanδ) of these giant dielectric oxides are one of their most serious drawbacks. Most recently, a promising giant dielectric oxide for future practical applications was reported in an In + Nb co-doped rutile–$TiO_2$ (INTO) ceramic [18]. INTO ceramics exhibited extremely high $\varepsilon'$ values of more than $10^4$, depending on the dopant concentration. Notably, tanδ of INTO ceramics was very low compared to those of other giant dielectric oxides. For example, doping $TiO_2$ with 10% (In + Nb) can result in values of $\varepsilon' \approx 6\times10^4$ and tanδ≈0.02 [18]. In addition to the models above, the electron – pinned defect – dipole (EPDD) model was suggested as an explanation of the fascinating giant–dielectric properties of INTO ceramics. According to the EPDD model, the aliovalent dopants used ($Nb^{5+}$ and $In^{3+}$) had a distinct function. The former, with higher valence state, was used to produce free electrons in the rutile–$TiO_2$ structure. The latter, with a lower valence state, was used to form local complex defect clusters that could confine free electrons [18]. It was further suggested that EPDDs can be produced in other co–doped $TiO_2$ systems [19,20]. This discovery has greatly stimulated research in the field of giant dielectric oxides [12,14,15,19–30]. In addition to the EPDD model,

* Corresponding author at: Department of Physics, Faculty of Science, Khon Kaen University, Khon Kaen 40002, Thailand.
*E-mail address:* pthongbai@kku.ac.th (P. Thongbai).

http://dx.doi.org/10.1016/j.jeurceramsoc.2017.04.040
0955-2219/

several studies have demonstrated that the giant dielectric properties of INTO ceramics originated from the IBLC or SBLC effect [13,15,23,25,27,29].

Several co–doped $TiO_2$ systems were synthesized and their giant dielectric properties reported. The aliovalent co–dopants studied were $Ga^{3+} + Nb^{5+}$ [12], $Bi^{3+} + Nb^{5+}$ [19], $Al^{3+} + Nb^{5+}$ [22], $Bi^{3+} + Sb^{5+}$ [30], and $Sm^{3+} + Nb^{5+}$ [20], among others. All of these co–doped $TiO_2$ systems showed very interesting giant dielectric behaviors. Various methodologies were used to clarify the origin of giant dielectric properties. From the point of view of capacitor applications, there is an ongoing need for a new system of co–doped $TiO_2$. Although the giant dielectric properties of many co–doped $TiO_2$ systems have been reported, we think that it is worthwhile to develop a new co–doped $TiO_2$ system to increase the number of design options and to support a variety of applications. Thus, in the current work, a new system of (Y + Nb) co–doped $TiO_2$ was synthesized. The phase composition and microstructure were carefully characterized. The giant dielectric and nonlinear current density–electric field (*J–E*) properties of (Y + Nb) co–doped $TiO_2$ ceramics were investigated. Interestingly, very large $\varepsilon'$ values were achieved in this new co–doped $TiO_2$ system. Interestingly, sintered ceramics can exhibit *J–E* characteristics. The origin of the giant dielectric response is also discussed in detail.

## 2. Experimental details

### 2.1. Ceramic preparation

$(Y_{1/2}Nb_{1/2})_xTi_{1-x}O_2$ ceramics with $x = 0.025$ and 0.05 (referred as 2.5%YNTO and 5.0%YNTO ceramics, respectively) were prepared using a combustion method with glycine as a fuel. $C_{16}H_{28}O_6Ti$ (Sigma–Aldrich), $Y(NO_3)_9{\cdot}6H_2O$ (Kento Chemical, >99.99%), $NbCl_5$ (Sigma–Aldrich, >99.9%), deionized water, citric acid, and glycine were used as the starting raw materials. Details of the preparation method are similar to those reported for preparation of $(In_{1/2}Nb_{1/2})_xTi_{1-x}O_2$ ceramics [15]. First, $Y(NO_3)_9{\cdot}6H_2O$ and $NbCl_5$ were dissolved in an aqueous solution of citric acid with constant stirring at room temperature (RT). Second, a $C_{16}H_{28}O_6Ti$ solution was added into the solution above until a clear and transparent solution can be observed. Third, glycine powder was mixed into the metal ion solution with stirring at 150 °C until a viscous gel was obtained. Then, the gel was dried at 350 °C for 1 h using heating rate 1 °C/min. Next, the resulting dried precursors were calcined in air at 1000 °C for 6 h. The powders obtained after calcination were pressed under uniaxial compression at ≈200 MPa into pellets that were 9.5 mm in diameter and ~1.5 mm in thickness. Finally, ceramic samples with dense ceramic microstructure and no porosity were achieved by sintering in air at 1500 °C for 2 h with heating and cooling rates 2 °C/min.

### 2.2. Characterizations

The phase composition and crystal structure of the ceramic samples were characterized using X–ray diffraction (PANalytical, EMPYREAN). The microstructure of sintered ceramics was characterized using field–emission scanning electron microscopy (FE–SEM) with energy–dispersive X–ray analysis (EDS) (HITACHI SU8030, Japan). The as – fired $(Y_{1/2}Nb_{1/2})_xTi_{1-x}O_2$ ceramics were carefully polished. Then, an obvious grain and grain boundary (GB) structure of the polished – samples was accomplished by thermally etching at 1100 °C for 30 min. Polished and etched surface was characterized by a scanning electron microscopy (SEM) (SEC, SNE4500 M). The chemical states of sintered $(Y_{1/2}Nb_{1/2})_xTi_{1-x}O_2$ ceramics were analyzed using X–ray Absorption Near Edge Structure (XANES) and X–ray photoelectron spectroscopy (XPS, PHI5000 VersaProbe II, ULVAC–PHI, Japan). XANES and XPS spectra were, respectively, collected at the SUT–NANOTEC–SLRI XAS beamline (BL5.2) (electron energy of 1.2 GeV; bending magnet; beam current 80–150 mA; 1.1 to 1.7 × $10^{11}$ photon $s^{-1}$) and at the SUT–NANOTEC–SLRI Joint Research Facility, the Synchrotron Light Research Institute (SLRI), Nakhon Ratchasima, Thailand. Detail of the XANES characterization technique are given elsewhere [31]. The XPS spectra were fitted with PHI MultiPak XPS software using a combination of Gaussian–Lorentzian lines.

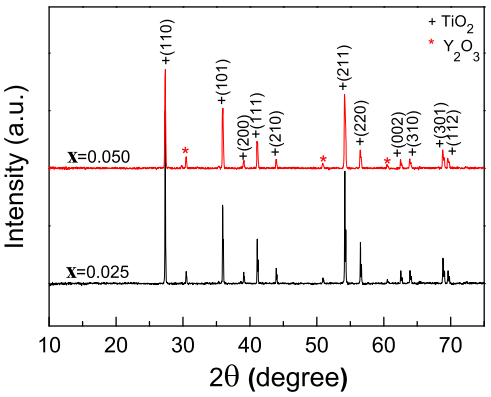


**Fig. 1.** XRD patterns of $(Y_{1/2}Nb_{1/2})_xTi_{1-x}O_2$ ceramics with $x = 0.025$ (2.5%YNTO) and 0.05 (5.0%YNTO).

### 2.3. Dielectric and electrical measurements

For dielectric and electrical measurements, Au was sputtered onto both pellet faces at a current of 25 mA for 8 min using a Polaron SC500 sputter coating unit. The capacitance ($C_p$) and dispassion factor (D or tanδ) were measured using a KEYSIGHT E4990A Impedance Analyzer over the frequency and temperature ranges of 40–$10^6$ Hz and −50–200 °C, respectively. Each measurement temperature was held constant with a precision of ±0.1 °C with an oscillation voltage of 0.5 V. The nonlinear current density–electric field (*J–E*) behavior at RT was measured using a high voltage measurement unit (Keithley Model 247). $E_b$ was defined as the electric field breakdown strength at which $J = 1$ mA/cm$^2$. The nonlinear coefficient (α) was calculated in the range of $J = 1$–10 mA/cm$^2$.

## 3. Results and discussion

Fig. 1 shows the XRD patterns of the sintered 2.5%YNTO and 5.0%YNTO ceramics. Both of the ceramic samples show a main phase consisting of rutile–$TiO_2$ (JCPDS 21–1276) with a tetragonal structure. A second phase of $Y_2O_3$ is observed in the XRD patters of these two samples. Lattice parameters (*a* and *c* values) were calculated. *a* values of the 2.5%YNTO and 5.0%YNTO ceramics are, respectively, 4.596 ± 0.001 and 4.598 ± 0.003, while *c* values are 2.963 ± 0.001 and 2.965 ± 0.003, respectively. The *a* and *c* values of both YNTO ceramics increase with increasing co–dopant concentration. Lattice parameters of both of the YNTO ceramics are larger than the *a* (4.593 Å) and *c* (2.959 Å) values of the pure rutile–$TiO_2$ (JCPDS 21–1276). The enhancement of the lattice parameters may be attributed to the larger ionic radii of $Y^{3+}$ ($r_6 = 0.90$ Å) and $Nb^{5+}$ ($r_6 = 0.64$ Å) than that of the host $Ti^{4+}$ ion ($r_6 = 0.605$ Å) [32]. With regard to the low dopant concentrations of $Nb^{5+}$ (1.25–2.5 at%) in both YNTO ceramics, $Nb^{5+}$ dopant ions can often completely enter into $Ti^{4+}$ sites in the rutile structure [18]. However, a secondary $Y_2O_3$ phase was detected indicating that some portion or all of the $Y^{3+}$ could not be substituted into the $Ti^{4+}$ sites. Considering the greatly increased *a* and *c* values, it is likely that only some portion of the $Y^{3+}$ ions were substituted into the $TiO_2$ structure.

Please cite this article in press as: T. Nachaithong, et al., Preparation, characterization, and giant dielectric permittivity of ($Y^{3+}$ and $Nb^{5+}$) co–doped $TiO_2$ ceramics, *J Eur Ceram Soc* (2017), http://dx.doi.org/10.1016/j.jeurceramsoc.2017.04.040